CONCEPTUAL DESIGN AND FEASIBILITY FOR A MINIATURE MARS EXPLORATION ROTORCRAFT

Noriaki TSUZUKI*, Shunichi SATO, Takashi ABE****
***University of Tokyo, **The Institute of Space and Astronautical Science**

Keywords: *Mars Exploration, Rotorcraft, Low Reynolds Number*

Abstract

An aerial vehicle operating under the command of a rover has a potential to extend the coverage for Mars exploration. Especially, a rotorcraft equipped with an imaging camera can gather geographic information around the rover and enables us to make a smart strategy for the exploration. In this paper, the feasibility for such a rotorcraft was assessed. For this purpose, the basic aerodynamic characteristics of rotors were experimentally investigated to assess a possible capability of the hover performance of the rotor in a very low Reynolds number regime that is due to the thin Mars atmosphere.

Nomenclature

AR	=	Rotor blade aspect ratio [2R/$c_{0.75R}$]
c	=	Rotor blade chord length (m)
$c_{0.75R}$	=	Rotor blade chord length at 0.75R (m)
C_T	=	Thrust coefficient [$T/\rho\pi R^2(\Omega R)^2$]
C_T/σ	=	Ratio of thrust coefficient to solidity
C_Q	=	Torque coefficient [$Q/\rho\pi R^2 R(\Omega R)^2$]
C_Q/σ	=	Ratio of torque coefficient to solidity
C_T/C_Q	=	Thrust to torque ratio
e	=	Hinge offset (m)
f/c	=	Maximum camber, in percentage of the chord
K_M	=	Torque constant of an electric motor (mNm/A)
M_{tip}	=	Mach number at the tip of a rotor
N_b	=	Number of blades
Q	=	Torque (Nm)
Re	=	Reynolds number based on $c_{0.75R}$ [$\rho c_{0.75R} U_{0.75R}/\mu$]
R	=	Rotor radius (m)
σ	=	(Thrust weighted) Solidity [$N_b c_{0.75R}/\pi R$]
T	=	Thrust (N)
$U_{0.75R}$	=	Flow velocity at 0.75R, tangent to the disk plane (m/s)
Ω	=	Rotation speed (rad/s)
θ_0	=	Collective pitch angle (deg.)
κ_{int}	=	Induced power factor from interference between upper and lower rotor of a co-axial rotor configuration [1]
ρ	=	Atmospheric density (kg/m^3)
μ	=	Atmospheric viscosity (kg/ms)
0.75R	=	75% of a rotor radius

1 Introduction

For the exploration of the planet such as Mars, the rovers such as Sojourner in the Mars Path Finder Mission or the Spirit and Opportunity in the Mars Exploration Rover Mission have played an active role for the in-situ surface exploration. The surface exploration in the present configuration by means of rovers, however, has various drawbacks and is expected to be improved in many ways for the future exploration. For instance, in the present configuration of the exploration by means of rovers, many time-consuming procedures are required for controlling the rovers; first, the geographical image around the rover is taken and is sent back to the commanding center on the earth,

second, based on the geographical image, the target site to where the rover is to move and the rough plan for rooting are decided and the commands giving those are sent back to the rover, third, the rover moves to the target site and takes the image around it. These procedures are repeated until the mission end. For transmitting the data, however, the transmission delay more than 10 minutes must be counted, and the distance to the target site is restricted since the information obtained from the geographical image taken by the rover is restricted and the longer the distance to the target site is, the larger the risk to which the rover will face becomes. In such a way, the planetary exploration by means of the rover system cannot be as efficient as we expect but remains much room to be improved.

To remove this drawback, we will propose to utilize a small aerial vehicle that will function as a scout for the sake of the rover. That is, the aerial vehicle will collect the geographical data around the rover, which is utilized to make a decision on the site to where the rover heads, then, the rover and the vehicle can make an autonomous exploration that does not need a redundant communication with the commanding center on the earth. The geographical data thus collected will give not only abundant information for the rover to make a smart strategy for the exploration, but also the fruitful scientific information that may be difficult for the rover to acquire by itself. The aerial vehicle for such a purpose should be a rotorcraft rather than a fixed-wing airplane since only the rotorcraft can land and take off from the arbitrary place with a restricted area. The development of such a rotorcraft, however, must solve some difficulty due to the thin Mars atmosphere. This is because the thin atmosphere causes a decrease of thrust that must be overcome by developing an efficient rotor. The aerodynamic characteristics of the rotor depend mainly on the Reynolds number (Re) that decreases due to the thin atmosphere. Therefore it is inevitable to develop a rotor as efficient as possible in a Reynolds number regime lower than that experienced by the conventional rotorcraft in the Earth atmosphere.

In the present paper, the feasibility for such a rotorcraft for Mars exploration will be investigated. For this purpose, the basic aerodynamic characteristics of rotors were experimentally investigated to access a possible capability of the hover performance of the rotor in a very low Reynolds number regime (Re=$10^3 \sim 10^4$) that is expected in the thin Mars atmosphere, and to draw up guidelines for designing an appropriate rotor in such a very low Reynolds number environment. Based on the guidelines for the rotor, the feasibility of such a rotorcraft for Mars exploration will be demonstrated.

2 Basic Aerodynamic Characteristics of Rotors in a Thin Atmosphere

2.1 Experimental Set-up

In order to directly assess the hover performance of the rotor, it is desirable to directly measure the aerodynamic characteristics of the rotor in its rotating state rather than to predict theoretically based on the characteristics of the 2D airfoil. Hence, the aerodynamic thrust generated by the rotor directly driven by an electric motor was measured. For this purpose, the drive motor, on which the rotor is directly attached, is directly mounted on the measurement stand. The measurement stand is composed of a pendulum, the inclination of which is proportional to the aerodynamic thrust. The experimental set-up for the measurement is depicted in Fig.1. The inclination of the pendulum was measured by the inclinometer (Midori-Precisions, PMP-S10LX). Prior to the measurements, the calibration curve for the thrust vs. the inclination angle was determined, which enable us to convert the measured inclination angle to the thrust generated by the rotating rotor. The electric motor to drive the rotor was a DC electric motor (Maxon Motor, RE25), of which rotation speed was measured by the installed tachometer. The output of the tachometer was 500 pulses per rotation. The torque required to rotate the rotor was measured based on the measurement of the electric current consumption to drive the electric motor, referring to a specific data of the motor on the relation be-

tween the torque and the electric current consumption (K_M). The measurements were carried out 3 times for each configuration and were averaged over to cancel the measurement error.

To simulate the thin atmosphere in Mars, the measurement system is mounted inside a large evacuation chamber of which diameter and height are 2.40 m and 2.73 m, respectively. In the present experiment, a primary scaling parameter for the rotor performance is the Reynolds number. The evacuation chamber enables us to adjust the Reynolds number simply. Other than the Reynolds number, it is expected that the rotation rate itself may affect the aerodynamic performance. The evacuation chamber enables us to examine this effect keeping the size of the rotor and the Reynolds number.

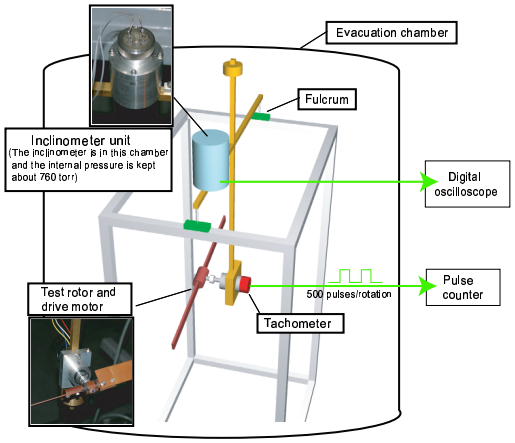

Fig. 1 Hover test pendulum. Output sensitivity of the inclinometer is less than 0.01 deg., which is equal to the thrust of 0.025 gf. Torque constant of the drive motor (K_M) is 23.18 mNm/A [2].

2.2 Rotor Models and Experimental Conditions

The rotor model is a single rotor and is composed of the hub attached with two symmetric blades having no twist angle. The specifications for the airfoil at the 75% of the rotor radius (0.75R) and the planform are depicted in Fig.2. Several combinations of the airfoil and the planform were investigated as shown in Table 1. The test conditions are summarized in Table 2. The Mach number at the tip of the rotor (M_{tip}) is 0.13 at most and, hence, the compressibility effect may be almost neglected.

Table 1 Test rotors. (All rotors are made of bakelite)

Rotor no.	Airfoil no.	Planform no.
A	1	a
B	2	a
C	3	a
D	4	a
E	5	a
F	6	a
G	7	a
H	1	b
I	1	c
J	1	d

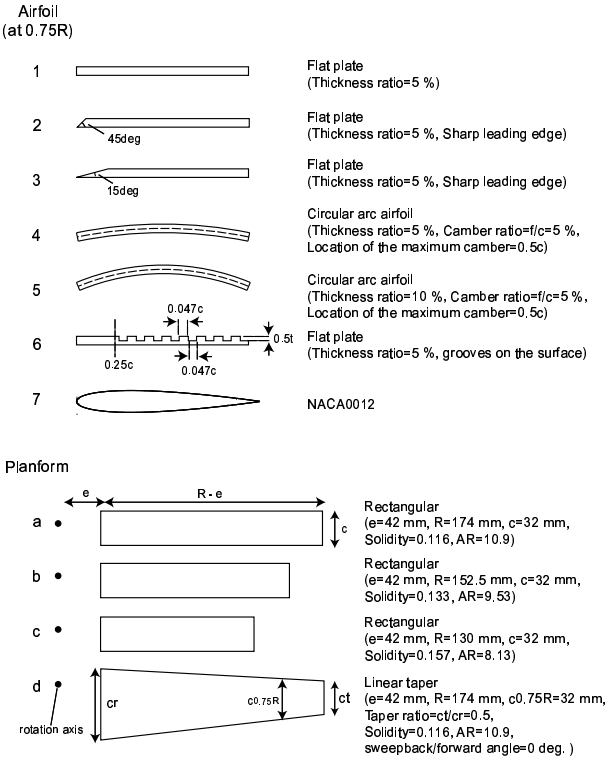

Fig. 2 Test airfoils and planforms.

Table 2 Test conditions.

Re	2000, 4000, 8000
M_{tip}	< 0.13
Test gas	Air
Collective pitch angle (θ_0)	0∼50 deg.

3 Experimental Results and Discussion

In the following subsection, the results for the measurement on the aerodynamic characteristics are described focusing on several features of the rotor configuration. In general, when comparing the performance of rotors with different blade areas, it is desirable to examine the ratio of thrust coefficient to solidity (C_T/σ) and the ratio of torque coefficient to solidity (C_Q/σ) in order to cancel the influence of the blade area on the thrust and the torque. Hence, the ratio of thrust coefficient to solidity and the ratio of torque coefficient to solidity, specifically, will be discussed.

For subsections from 3-1 to 3-5, the extent of measurement error for C_T/σ and C_Q/σ are within the size of the symbol mark in the figures, and the Reynolds number and the rotation speed are fixed as 4000 and 600 RPM, respectively.

3.1 Effect of Sharpness of the Leading Edge

The rotor hover performances for various sharpness of the leading edge are presented in Fig.3. For a leading edge with a sharpness of 45 deg., we can observe the improvement on the hover performance; the increase of C_T/σ and the decrease of C_Q/σ, while this improvement is deteriorated for a leading edge with further sharpness. Therefore we can conclude that the appropriate sharpness of the leading edge is effective to improve the rotor hover performance.

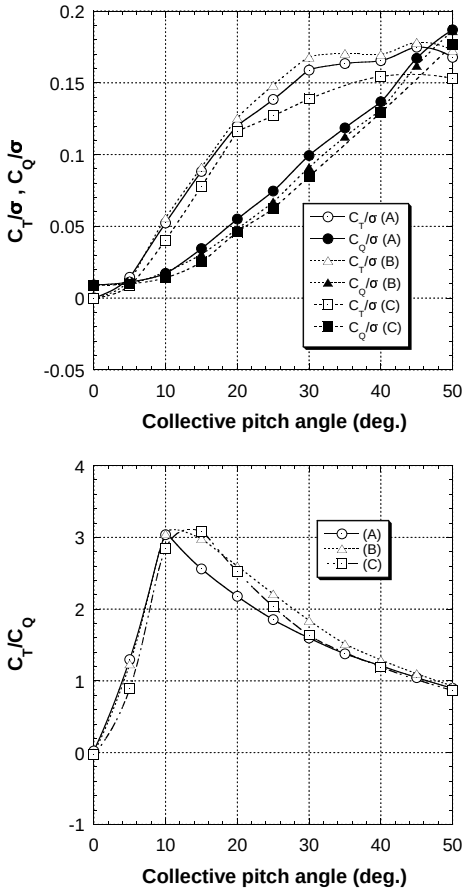

Fig. 3 Effect of sharpness of the leading edge on above) ratio of thrust and torque coefficient to solidity and below) thrust to torque ratio. (Re=4000, rotation speed=600 RPM)

3.2 Effect of Camber

The rotor hover performances for various cambers are presented in Fig.4. When the camber (f/c) increases, not only C_T/σ but also C_Q/σ increase. In addition, for a blade of which camber is 5 %, we can observe the improvement on the thrust to torque ratio (C_T/C_Q) for θ_0<10 deg., while this improvement is deteriorated for a blade with further camber. For θ_0>10 deg., in contrast, as the camber increases, C_T/C_Q increases. Therefore we can conclude that; first, a camber for the blade is quite effective to increase the thrust, second, for small collective pitch angles the appropriate camber for the blade is effective to improve the rotor hover efficiency, while for high collective pitch angles the efficiency increases with the camber.

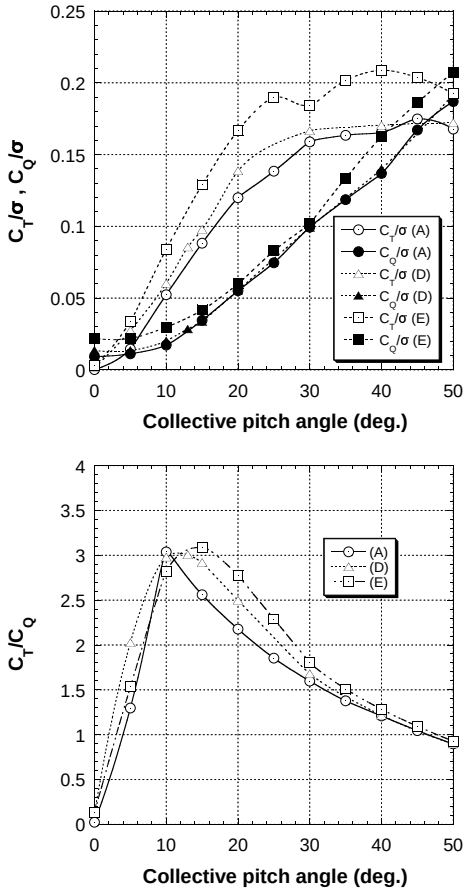

Fig. 4 Effect of camber on above) ratio of thrust and torque coefficient to solidity and below) thrust to torque ratio. (Re=4000, rotation speed=600 RPM)

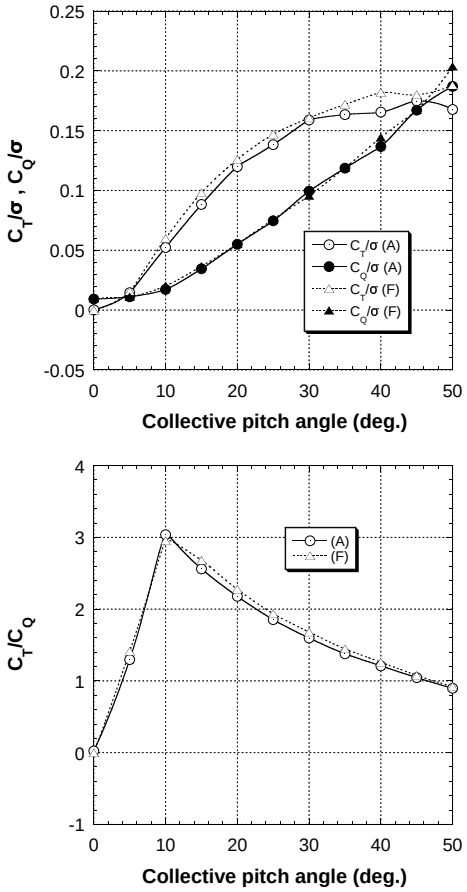

Fig. 5 Effect of grooves on the blade surface on above) ratio of thrust and torque coefficient to solidity and below) thrust to torque ratio. (Re=4000, rotation speed=600 RPM)

3.3 Effect of Grooves on the Blade Surface

In the lower Reynolds number regime, the skin friction on the blade surface may play a significant role in the torque force required to rotate the rotor. The grooves on the surface of the blade were intended to decrease the friction. The rotor hover performance of the blade with grooves on the surface was improved in that it increases C_T/σ and C_Q/σ is remained to be unchanged, as presented in Fig.5. It is expected that the expected decrease of C_Q/σ may be cancelled out by its increase due to the increase of C_T/σ. In any event, in a viewpoint of manufacturing the blade, the grooves on it may enable us to reduce mass of the blade.

3.4 Effect of Aspect Ratio

The influence of aspect ratio (AR) on the rotor hover performance is depicted in Fig.6. When the aspect ratio increases, not only C_T/σ but also C_Q/σ increase while C_Q/σ remains to be unchanged for a smaller collective pitch angle: θ_0 <15 deg.. The increase of the torque may be caused by the increase of the viscous part of the drag, which becomes dominant in the lower Reynolds number regime. Nevertheless, the hover efficiency (C_T/C_Q) increases with aspect ratio due to the increase of C_T/σ.

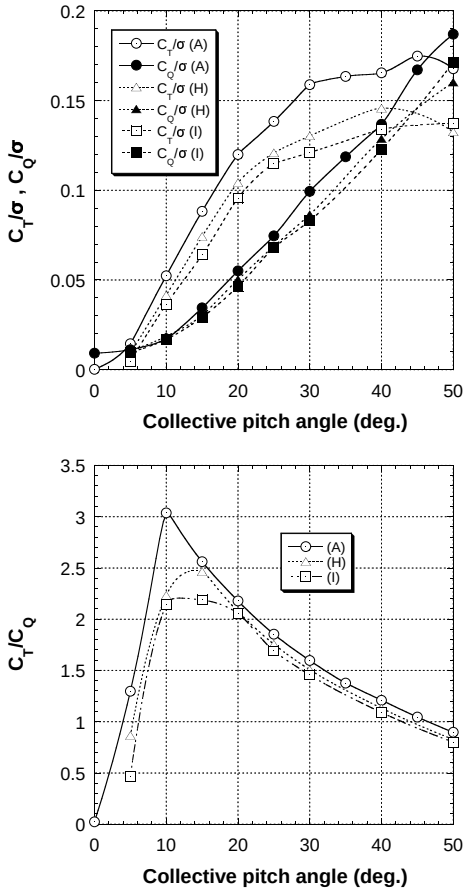

Fig. 6 Effect of aspect ratio on above) ratio of thrust and torque coefficient to solidity and below) thrust to torque ratio. (Re=4000, rotation speed=600 RPM)

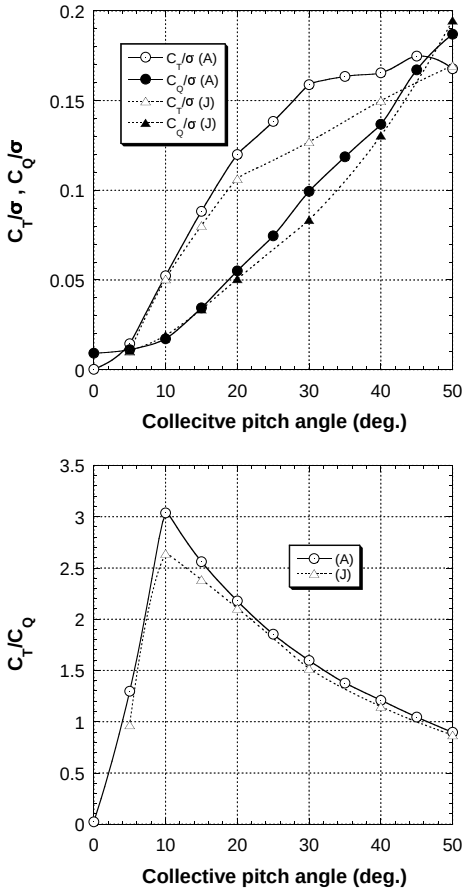

Fig. 7 Effect of the tapered planform on above) ratio thrust and torque coefficient to solidity and below) thrust to torque ratio. (Re=4000, rotation speed=600 RPM)

3.5 Effect of the Tapered Planform

In the present configuration, the tapered planform is designed based on the rectangular planform so that they have an identical aspect ratio and lifting line. According to Fig.7, the tapered planform has less effective characteristics not only in C_T/σ but also in C_T/C_Q.

3.6 Effect of Reynolds Number

The effect of Reynolds number is represented in Fig.8 for the typical rotor. When the Reynolds number increases, C_T/σ increase as expected. C_Q/σ, however, slightly decrease for θ_0<15 deg. while it increases for θ_0>15 deg. The increase of C_Q/σ may be caused by the induced drag.

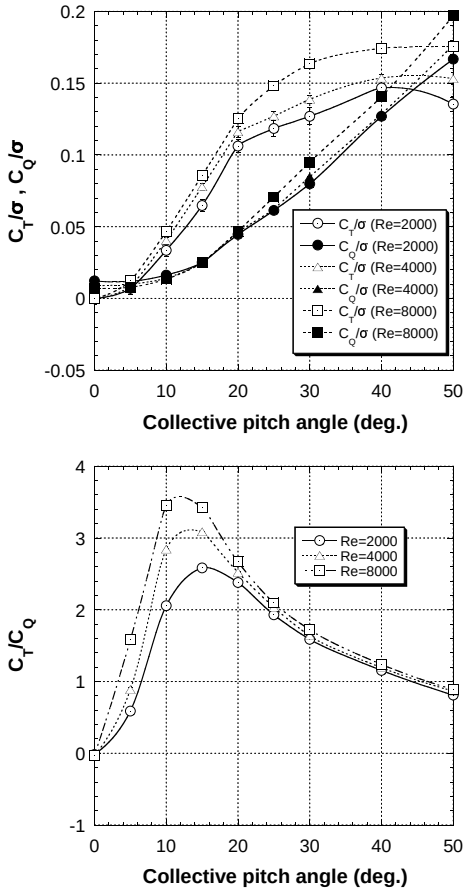

Fig. 8 Effect of Reynolds number on above) ratio of thrust and torque coefficient to solidity and below) thrust to torque ratio of the rotor(C). (Rotation speed=600 RPM)

3.7 Effect of Rotation Speed

The aerodynamic characteristics of the rotor are considered to be dominated by the Reynolds number. To confirm this fact, we compare the aerodynamic characteristics of the rotor with identical Reynolds number but with different rotation speed as shown in Fig.9. No meaningful effect was not observed for θ_0<20 deg., while there is slight difference for θ_0>20 deg.

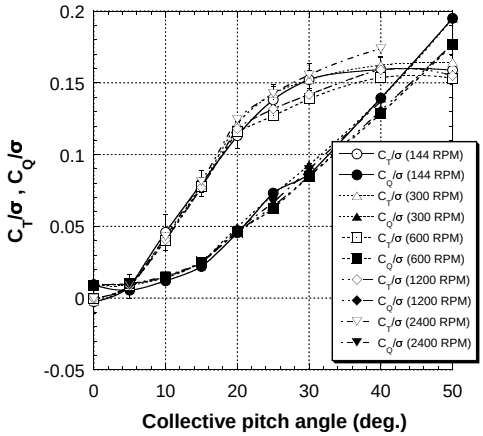

Fig. 9 Effect of rotation speed on the measured hover performance of the rotor(C). (Re=4000)

4 Applicability of LMT

For the feasibility study of the rotorcraft as will be done later, it is necessary to know the aerodynamic performance for many specific rotors that are selected in the design process. For this purpose, it is useful if we can predict it by means of the existing theory such as Local Momentum Theory (LMT) [4]. In this section, we will examine the applicability of the LMT in the lower Reynolds number regime like in the present paper. To this aim, we will compare the present experimental data with the prediction by the LMT. This comparison not only shows an applicability of LMT but also will suggest the possible flow mechanism explaining the difference between them if any.

Figure 10 shows a comparison of the LMT with the experimental result for the typical rotor at Re=4000. Note that for small collective pitch angles until around 10 deg., the agreement is good enough for a preliminary design of the vehicle. For θ_0>15 deg., however, there is a serious underprediction of both C_T/σ and C_Q/σ because of the stall delay phenomena due to the three-dimensional effect, while we cannot observe such an obvious stall delay on the rotor of which airfoil is a stream line leading edge as in Fig.11. Therefore, we believe that the stall delay and high-thrust generation at high collective pitch angles as in Fig.10 was caused by mainly

the leading edge vortex (LEV), which is facilitated by a sharper configuration of the leading edge. Since it is believed that insects have succeeded in flight in the very low Reynolds number regime (Re=10^3～10^4) exploiting the high-lift generation mechanism caused by the LEV [7], the present experimental result suggests that there is a possibility to enhance the rotor performance by utilizing the features of the insect wing.

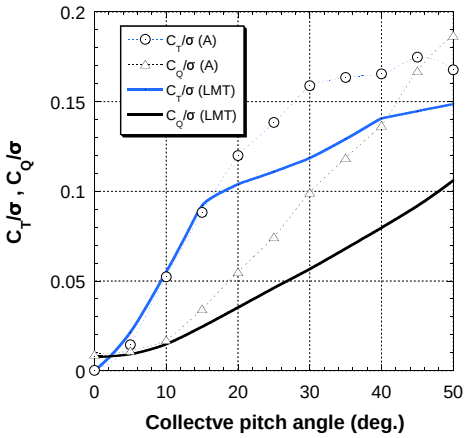

Fig. 10 Measured and predicted hover performance on the rotor(A). (Re=4000, rotation speed=600 RPM). Source of the 2D airfoil data at Re=4000: reference [5].

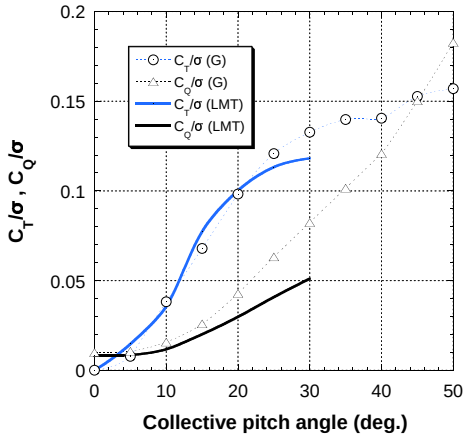

Fig. 11 Measured and predicted hover performance on the rotor(G). (Re=4000, rotation speed=600 RPM). Source of the 2D airfoil data at Re=4000: reference [6].

Even though the theoretical prediction shows a difference with the experimental result especially at larger collective pitch angles, it agrees with the latter reasonably at the smaller collective pitch angles. Therefore, we will apply the LMT to predict the aerodynamic performance of the rotor for the purpose to access the feasibility of the rotorcraft in Mars atmosphere.

5 Feasibility Analysis for the Rotorcraft in a Thin Mars Atmosphere

The rotorcraft under consideration is to operate together with the rover and, therefore, should be small as possible. Even though several tasks are possible for the vehicle, we will consider the mission in which only the geographical picture is to be taken and to send it to the rover. In the present analysis, we assume the vehicle of mass of 100 g, which may be a minimum mass including a structure, a rotor, a drive motor system, a power source system, a telecommunication system, and an imaging camera. A simple estimation for mass expected for each components except the drive motor system and its power source system gives the total mass of around 60 g all together as summarized in Table 3. Hence the total weight allocated for the drive motor system and its power source system is around 40 g.

For the configuration of the rotor, we assume a co-axial configuration that is suitable for the present small vehicle since it enable us to eliminate the tail rotor and to minimize the requirement for the vehicle. Since the gravity on the Mars is about 37.3 % of that on the Earth [3], the present rotor must generate a thrust of 37.3 gf, at least, to lift off. For the rotor size and the rotation speed specified appropriately, the power consumption is determined for a set of required C_T/σ and C_T/C_Q to hover, then, we can draw a curve of constant power consumption on the chart of C_T/σ vs. C_T/C_Q as in Fig.12.

According to the specification of the commercially available batteries, the power-to-mass ratio is limited as less than 0.2 Wh/g. That is, the maximum electric energy attainable by the total mass of 40 g for the motor system and its power source system cannot exceed 8 Wh. Therefore, when the flight endurance is required to be 15 minutes for instance, the power consumption is limited

as less than 32 Watts. In Fig.12, several curves for the power consumption of 32 Watts are drawn for 0.15, 0.30, and 0.50 m of rotor radius, based on the rotor in Table 4. Considering the packaging space for the aerial vehicle and the rigidity of the blade, however, rotor radius is assumed to be limited as less than 0.50 m. On the other hand, according to the present experimental results, attainable values for C_T/σ and C_T/C_Q are less than 0.2 and 5, respectively. These boundaries are depicted on the chart of C_T/σ vs. C_T/C_Q as in Fig.12. Therefore, the region enclosed by the curves for the power consumption of 32 Watts, the lines of 0.2 and 5 for C_T/σ and C_T/C_Q are allowed for designing the vehicle. According to the figure, there still remains a region for the design point even though not large, and we can expect the increase of the region with the rotor radius.

Now, let us assume, for instance, the co-axial rotor configuration as described in Table 5. The LMT predicts C_T/σ and C_T/C_Q as 0.95 and 3.8, respectively. This rotor performance can generate a thrust of 38 gf that is enough to lift off and consumes a power of 12.7 Watts to rotate the blades at 2360 RPM. It should be noted that, for this rotor, the Reynolds number is 2500 and the Mach number at the tip of the blade is 0.25. Those conditions do meet the applicability of the prediction. According to Fig.13, this rotor performance is within the design criteria. Based on the consumption power of 12.7 Watts, the minimum battery mass is expected as 16 g and the remaining mass of 24 g out of 40 g can be allocated to the mass of the electric motor. This estimation may not be realized by the off-the-shelf technologies. However, taking into account of the improvement on the continued advancement in micro technology, it is reasonable to take this estimation as a design guideline. On the other hand, as listed in Table 3, the present rotor is expected to be manufactured keeping its mass within 12 g.

The rotor system assumed in Table 5 is not elaborated to the limit but there is plenty room for improvement. Therefore, taking into account of the improvement on the rotor performance and the continued advancement in micro technology, we can expect the rotorcraft to fly in the Mars atmosphere in the near future.

Table 3 Estimation for mass of components of the rotorcraft except a driving motor system and its power source system.

Control unit and battery	11 g
Telemeter and battery	8 g
Imaging camera, transmitter and battery	15 g
Rotor (blades and hubs)	12 g
Fuselage	10 g
Total	56 g

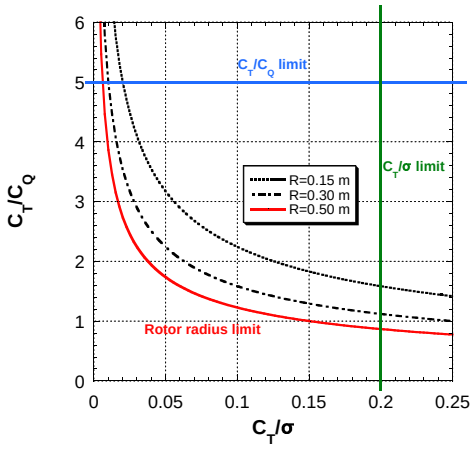

Fig. 12 Chart of the design criteria (I). The curves on this chart mean the constant power consumption rate of 32 Watts, which is the maximum total power requirement to the power system. The motor and gearbox efficiency is supposed to be 80 % and 70 %, respectively.

Table 4 Details of the co-axial rotor for Fig.12.

Planform	Rectangular, c=0.030 m
Root cutout ratio (e/R)	20 %
Number of blades	4

Table 5 Details of the co-axial rotor at the design point in Fig.13.

Rotor radius	0.30 m
Airfoil	No.1 in Fig. 2
Planform	Rectangular, c=0.030 m
Root cutout ratio (e/R)	20 %
Number of blades	4
Collective pitch angle (θ_0)	12 deg.
Twist pitch angle	0 deg.
Induced power factor (κ_{int}) [1]	1.16

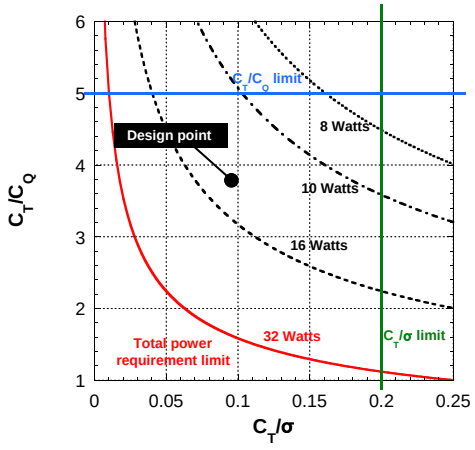

Fig. 13 Chart of the design criteria (II), based on the rotor in Table 5. The motor and gearbox efficiency is supposed to be 80 % and 70 %, respectively.

6 Conclusion

The feasibility of the rotorcraft in the Mars atmosphere of which mass is a 100g class was investigated and the design guideline was presented. The design guideline shows that, even though the off-the-shelf technologies cannot satisfy all the design guideline, we can expect the feasibility of the rotorcraft, taking into account of the improvement on the rotor performance and the continued advancement in micro technology. Especially for the improvement of the rotor performance, the basic guidelines were supplied experimentally. That is, the guidelines for designing a efficient rotor in a very low Reynolds number regime (Re=10^3～10^4) can be summarized as follows;

1) An appropriate sharp leading edge is effective.
2) A camber is quite effective to increase the thrust, and an appropriate camber is effective to improve the hover efficiency for small collective pitch angles, while for high collective pitch angles the efficiency increases with the camber.
3) The aspect ratio should be as small as possible.
4) The taper is not effective on the hover performance under the condition that the aspect ratio and the lifting line are both identical with those of the rectangular planform.
5) The Reynolds number should be as high as possible.
6) The lightweight blade may be possible to modify the airfoil surface to be grooved for instance.

References

[1]J. G. Leishman., *Principles of helicopter aerodynamics*., Cambridge University Press, New York, NY, 2000, pp. 69-71.

[2]Maxon motor., Products catalog., http://www.maxonmotor.com/

[3]A. Datta et al., "Design of a Martian Autonomous Rotary-Wing Vehicle"., *Journal of aircraft*, Vol. 40, No. 3, 2003, pp. 461-472.

[4]A. Azuma and K. Kawachi., "Local Momentum Theory and Its Application to the Rotary Wing"., *Journal of aircraft*, Vol. 16, No. 1, 1979, pp. 6-14.

[5]S. Sunada et al., "Unsteady Forces on a Two-Dimensional Wing in Plunging and Pitching Motions"., *AIAA journal*, Vol. 39, No. 7, 2001, pp. 1230-1239.

[6]S. Sunada et al., "Comparison of Wing Charcteristics at an Ultralow Reynolds Number"., *Journal of aircraft*, Vol. 39, No. 2, 2002, pp. 331-338.

[7]H. Liu and K. Kawachi.,"A Numerical Study of Insect Flight"., *Journal of computational physics*, Vol. 146, 1998, pp. 124-156.